Journal of Glaciology, Vol. 49, *No.* 167, 2003

Glacier surge mechanisms inferred from ground-penetrating radar: Kongsvegen, Svalbard

JOHN WOODWARD,[1] TAVI MURRAY,[2] ROGER A. CLARK,[3] GRAHAM W. STUART[3]
[1]*Division of Geography, Northumbria University, Lipman Building, Newcastle-upon-Tyne NE1 8ST, England*
E-mail: john.woodward@northumbria.ac.uk
[2]*School of Geography and* [3]*School of Earth Sciences, University of Leeds, Leeds LS2 9JT, England*

ABSTRACT. Deformational structures at the surge-type glacier Kongsvegen, Svalbard, are displayed at the glacier surface and on a grounded cliff section at the terminus. A 300 m × 65 m grid of 200 MHz ground-penetrating radar (GPR) profiles has been collected adjacent to the cliff section in order to identify englacial structure. Two sub-horizontal reflectors have been imaged; the upper is interpreted as the glacier bed, and represents a transition between glacier ice and frozen subglacial sediments; while the lower is interpreted as a transition between frozen and unfrozen subglacial sediment. Dipping reflectors, corresponding to sediment-filled features on the cliff and glacier surface, do not cross the glacier bed. A small number of reflectors, interpreted as thrust faults, are visible below the bed reflector. A model is developed for structural development, which suggests that ice built up in a reservoir zone during quiescence. During the surge, ice propagated rapidly from this reservoir, creating a zone of compression which resulted in thrusting. Subsequently an extensional flow regime resulted in extensive fracture of the ice. We suggest dilated sediment was evacuated into these extensional crevasses from the glacier bed, accelerating surge termination.

INTRODUCTION

Surge-type glaciers oscillate between periods of rapid movement and periods of relative inactivity or quiescence (Post, 1969). The exact mechanisms driving this flow instability are not fully understood, though recent studies suggest that surging is likely a result of: changing conditions in the sediments at the ice–bed interface (e.g. Clarke and others, 1984); changing thermal conditions (e.g. Robin, 1955; Clarke, 1976; Fowler and others, 2001); and/or changing hydrological conditions (e.g. Kamb, 1987). What is increasingly apparent is that the complexities of surge initiation, the mechanisms for sustaining fast flow and surge termination cannot all be explained by any single model. To understand better the dynamics of surge-type glaciers, more direct observations are needed of the surge cycle for a range of surging glaciers. This is particularly difficult in remote areas, where surges are difficult to monitor, and in Arctic areas, where the period of quiescence is often >150 years (Dowdeswell and others, 1991). Alternative methods must be developed to investigate the development and termination of surges in such areas. A number of studies have attempted to identify surge-type glaciers using diagnostic sedimentary structure in the glacier body and the glacier forefield (e.g. Sharp, 1985; Evans and Rea, 1999). If certain sedimentary structures can be uniquely linked to different phases of the surge then identification of these structures may allow us to recognize different modes of surging. The problem is that sedimentary structures are only available for study at the glacier surface and at the glacier front. Ground-penetrating radar (GPR) is one method for extending the study area to permit suites of structure to be identified within the ice matrix.

GPR is a geophysical technique developed for the non-invasive investigation of subsurface features. Electromagnetic wave energy from a transmitter unit on the ground surface is partially reflected from subsurface features exhibiting electrical properties contrasting with those of the surrounding matrix (Daniels and others, 1988). In glacier ice, marked contrasts in electrical properties are a result of changes in the temperature of the ice (e.g. where a warm ice layer exists below cold surface ice (Björnsson and others, 1996)), changes in water content (Murray and others, 2000a, b), changes in bubble content of the ice (Macheret and Zhuravlev, 1982), changes in the chemical composition of the ice (Gudmandsen, 1975), or varying debris concentration in the ice (e.g. Arcone and others, 1995). Radar can also be used to map features formed as a result of brittle fracture in the ice, such as crevasses (e.g. Jezek and others, 1979; Glover and Rees, 1992), faults (Murray and others, 1997) and shear zones (Nobes and others, 1994).

Few GPR surveys have been carried out to investigate structures produced by the incorporation of sediments in surge-type valley glaciers. One glacier that has been studied is Bakaninbreen, Svalbard. Basal and englacial sedimentary features were mapped, many of which were interpreted to be sediment-filled thrust features 0.6–1.1 m thick, although displacement could only be demonstrated across one feature (Murray and others, 1997, 2000b). Some of these englacial features correspond to surface outcrops mapped by Hambrey and others (1996), and they appear to transport considerable volumes of sediment from the basal zone (Murray and others, 2000b).

https://doi.org/10.3189/172756503781830458 Published online by Cambridge University Press

Previous investigations at the surge-type glacier Kongsvegen, Svalbard, have identified suites of englacial sedimentary structures. How this sediment is incorporated into the ice is currently unresolved. It could be by thrusting (Bennett and others, 1996; Hambrey and others, 1999), folding sub-parallel to glacier flow (Glasser and others, 1998; Hambrey and others, 1999) or crevasse filling (Woodward and others, 2002). This paper details GPR investigations of the sediment structures near the terminus of Kongsvegen. GPR results will be used to develop models of sediment emplacement and models for the surge of Kongsvegen. First, the ability of GPR to image structure in the ice of Kongsvegen will be investigated. Second, mechanisms for the development of the structure identified using GPR will be developed. These mechanisms will then be used to construct a model for surge initiation, the period of fast flow and then surge termination.

FIELD SITE

Kongsvegen (78°48′ N, 12°59′ E) is a 27 km long, 189 km^2 surge-type glacier in northwest Spitsbergen (Hagen and others, 1993) (Fig. 1), which currently terminates in a partially grounded and partially calving front. The grounded section of the front forms a cliff face 5–20 m high running northwest–southeast for >1 km along the fjord margin (at 160–185° to the ice-flow direction). The glacier surface profile parallel to the cliff face dips at ~2° along the fjord, and in its lower reaches is almost horizontal perpendicular to the ice cliff. The calving margin of Kongsvegen is confluent with the principal flow unit of Kronebreen and Infantfonna at the head of Kongsfjorden. During periods of advance, the complex is confluent with another stream of Kronebreen to the north of Collethøgda. The Kongsvegen flow stream is currently quiescent, with a flow rate of ~3 m a^{-1} (Melvold and Hagen, 1998). By contrast, Kronebreen is currently one of the fastest-flowing tidewater glaciers in Svalbard, with a flow speed of ~750 m a^{-1} (Lefauconnier and others, 1994; Melvold and Hagen, 1998).

Interpretation of aerial photographs suggests that the last surge of Kongsvegen occurred between 1936 and 1956 (Woodward and others, 2002). Oblique aerial photographs from 1936 show the catchment in a pre-surge state, with the medial moraine complex separating Kronebreen from Infantfonna and Kongsvegen close to the Botnfjellbreen margin of Kongsvegen, as it is today. By comparison, the 1948 photograph shows a wider and more heavily crevassed Kongsvegen flow unit. The 1948 photograph also shows the maximum recorded advance of the tidewater margin, thought to be a result of the push effects of the advance of the surge front propagating down the Kongsvegen flow unit (Woodward and others, 2002). By 1956 the Kongsvegen flow unit covered two-thirds of the joint tidewater margin. Subsequently the tidewater complex has retreated, Kongsvegen has entered quiescence and Kronebreen has gradually widened to almost completely squeeze out the Kongsvegen tongue (Melvold and Hagen, 1998).

METHODOLOGY

Data collection

A grid of 200 MHz GPR lines was collected along the margin of Kongsvegen during July 1996 (Fig. 1) using a Pulse EKKO 100 GPR system. Two types of survey were undertaken, common-offset (CO) and common-midpoint (CMP). During CO surveys the antennae, fixed perpendicularly to the survey line on a plastic sledge, were moved progressively along the profile in step mode, collecting traces at 0.25 m intervals along the profile. During CMP surveys, the antennae were moved progressively further apart at an equal offset from the central image point. Reflections from CMP surveys were used to calculate the velocity of propagation of electromagnetic energy in the subsurface. This allows a depth scale to be added to processed survey lines. Three 300 m long parallel lines, approximately 11 m apart, were collected parallel to the grounded cliff face at the glacier terminus. These lines are denoted low line (LL), mid-line (ML) and upper line (UL) (Fig. 1b). Five cross-lines, each approximately 65 m long, were also surveyed, spaced every 55 m. These lines are denoted XLA–XLE. During data collection, the locations of surface water and streams, and the angle at which any visible trace or sediment-filled fracture

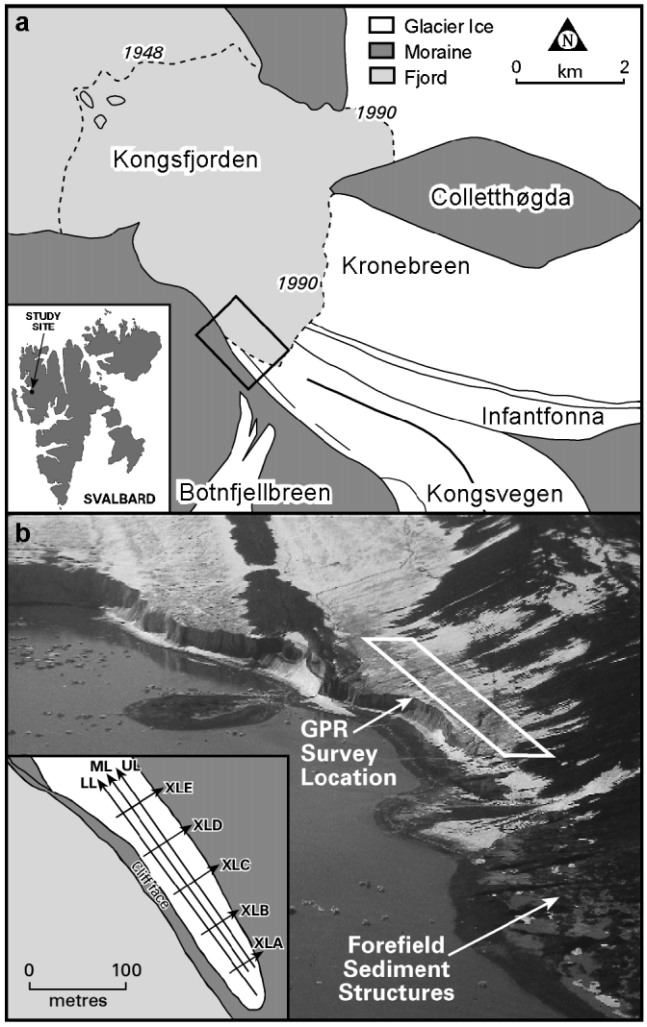

Fig. 1. (a) The tidewater margin of Kongsvegen, Svalbard, showing the position of the margin from 1948 and 1990 aerial photographs and the current dominance of Kronebreen at the tidewater margin. The box marks the location of the photograph shown in (b). (b) Oblique photograph, with the location of the GPR grid marked. The grounded cliff face running along the margins of Kongsfjorden and the proglacial sediment structures in the marginal area of Kongsvegen are visible. The inset box shows details of the GPR grid, arrows marking the direction of survey for each of the lines.

https://doi.org/10.3189/172756503781830458 Published online by Cambridge University Press

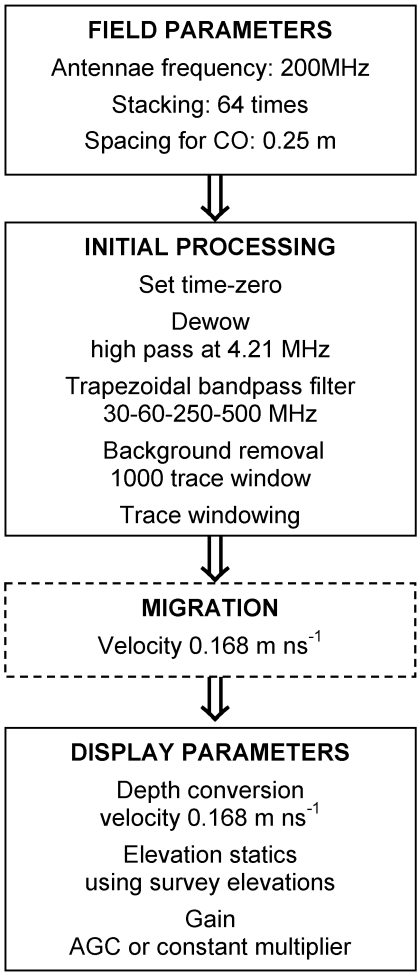

Fig. 2. Processing flow for GPR data. A description of processing parameters is given in the text. Migration has not been applied to all GPR profiles.

crossed the GPR lines, were noted, along with the location of the structure, and where possible an estimate of its dip.

GPR profiles were processed using GRADIX 1.10 software (Interpex Ltd). The processing sequence was optimized using CO profile LL (Fig. 2), then applied to all profiles. Drift correction and time-zero correction were applied, followed by dewow (4 MHz highpass) and bandpass filtering (trapezoidal filter set at 30–60–250–500 MHz) to remove noise at the high and low ends of the spectrum. Background removal in a window of 1000 traces was applied to remove coherent horizontal banding from the radar profile. Gain (either a constant gain or a time-varying automatic gain adjusted within 40 ns blocks) was applied to enhance returns from deeper reflectors whose signal strength is diminished by losses from attenuation, geometric spreading, scattering and energy partitioning at shallow interfaces. Depth and elevation correction allow the finished output to match surface topography with a true depth scale.

Reflections from near-horizontal layers were identified from CO profiles, and these reflectors were then picked manually from CMP surveys. This allowed calculation of radar wave velocities of 0.168 ± 0.002 m ns^{-1}. CMP velocities were used to apply depth and elevation corrections.

All profiles were also migrated using an F-K migration algorithm with a constant velocity of 0.168 m ns^{-1}, though not all profiles in this paper are displayed with migration applied. As the GPR grid was not dense enough for the reliable application of three-dimensional migration algorithms, GRADIX's two-dimensional algorithm was used, which assumes all energy is returned from in-line reflectors. However, the profiles did not cross all features at 90° to their trend, thereby violating the two-dimensional assumption. Furthermore, the velocity of 0.168 ± 0.002 m ns^{-1} was derived from propagation in cold ice, and is therefore inappropriate for migrating parts of the profile containing sediments or warm ice. GRADIX supports migration using only one-dimensional velocity models, but the dominant reflectors are not horizontal, and lateral variations in velocity are evidently present. Thus migration has not always successfully focused the reflection images where there are apparently large volumes of included sediment, or in the deeper (warmer) parts of the section.

RESULTS

The GPR profiles can be divided into three distinct sequences by two high-amplitude, sub-horizontal reflectors denoted SHR1 and SHR2 (Fig. 3). On LL, ML and UL, SHR1 dips up-glacier at ~3° and has opposite phase to the direct wave, indicating a higher dielectric permittivity (lower velocity) for the layers below the reflector than for those above it. The reflector is continuous except for occasional small steps in the profile and disturbances where steeply dipping structures rise from the reflector (e.g. at 93.3–96.5 m on LL). On the cross-lines XLA and XLB the reflector dips towards the fjord at 3–5°, less steeply than the trend of the glacier surface. On XLC–XLE the reflector dips towards the fjord at a slightly steeper angle, > 5°, and is approximately parallel to the surface.

The second sub-horizontal reflector, SHR2, also dips down-glacier at 0.5–3.5° and has opposite phase to the direct wave. From 0 to 80 m on the up-glacier orientated lines, the reflector is discontinuous and appears to be made up of a number of sub-parallel reflectors. From 80 to 240 m the reflector is more continuous and more steeply dipping, before again becoming somewhat discontinuous after 240 m as the layer rises to meet and merge with SHR1. On XLA–XLD the reflector dips towards the fjord parallel to the general trend of the glacier surface. On XLE the reflector is barely visible but seems to be slightly below SHR1.

The near-surface region of all the profiles is dominated by shallow diffraction patterns, which originate at the glacier surface and produce scatter (noise) on the GPR profile (Fig. 3). Some of these features appear to be symmetric and migrate successfully, while others are asymmetric and cannot be migrated successfully, leaving migration "smiles" and residual noise as the most obvious signal of the shallow structures in migrated sections.

The section of the lines below the near-surface and above SHR1 is dominated by asymmetric diffraction patterns suggesting steeply dipping structures, occurring every 10–15 m, and similar to those shown in Figure 4. Before migration, these reflectors seem to stem from a diffraction pattern with a straight limb on the up-glacier side. Below the diffraction pattern are a series of hyperbolae running towards the bed. When migrated, the upper hyperbola becomes a point reflector with a steeply dipping linear structure running from the point reflector towards the bed (Fig. 4a). The linear part of the reflector has moved up-dip

https://doi.org/10.3189/172756503781830458 Published online by Cambridge University Press

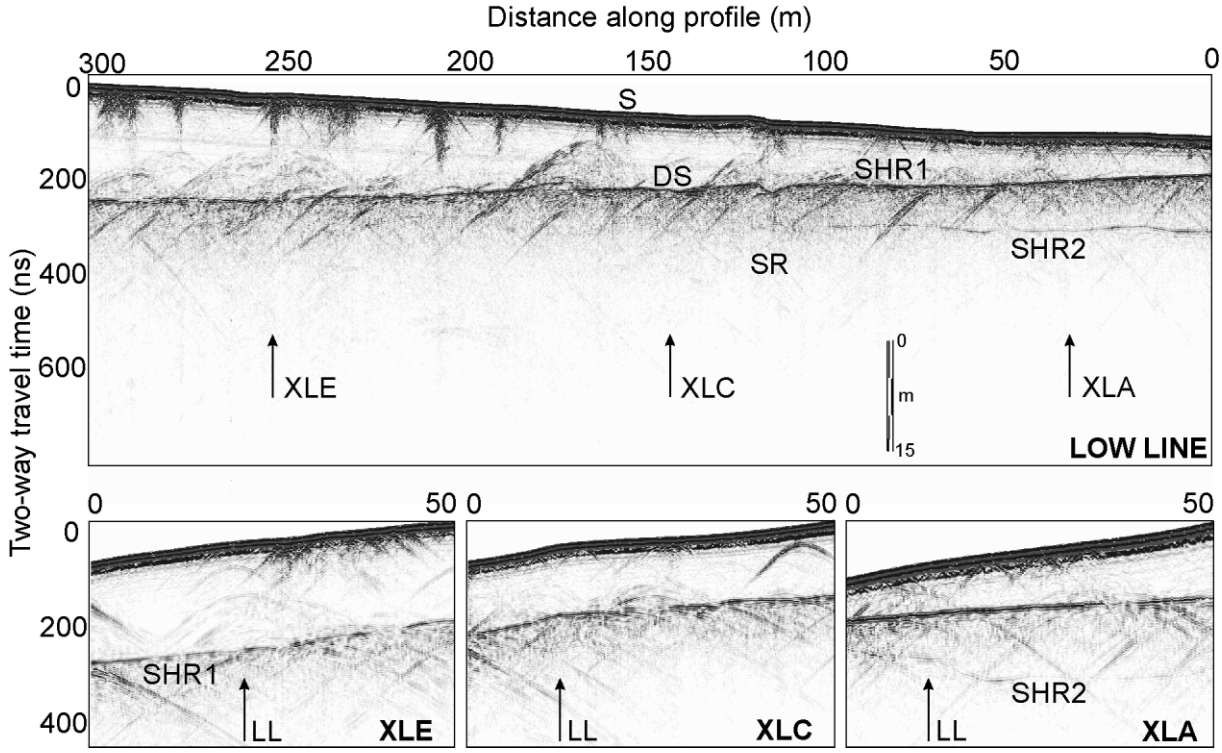

Fig. 3. GPR profiles collected from the grid shown in Figure 1. The low line (LL) and the three cross-lines XLA, XLC and XLE are displayed. Processing parameters are as recorded in Figure 2, though profiles are unmigrated and have constant gain. Two prominent sub-horizontal reflectors, SHR1 and SHR2, are identified on LL, as are surface scatter (S), dipping structures above SHR1 (DS) and shallow reflectors (SR) below SHR1. Flow direction is from left to right for LL, and out of the page for XLA, XLC and XLE. The depth-scale bar (in m) on LL applies to all parts of the figure.

and steepened considerably. The hyperbolae collapse to point reflectors along the plane of the structure. After migration, features do not appear to cross SHR1, while migration smiles below the reflector are a common feature, presumably due to the difficulties of the constant velocity model as described above, or because the reflections from the structures are not truly hyperbolic.

Below SHR1 a series of shallow, 20–30°, up-glacier dipping structures are apparent, which continue below SHR2. A number of structures, such as that dipping up-glacier from 104 m on LL, are visible before migration and remain prominent post-migration (Fig. 5).

INTERPRETATION OF STRUCTURE IN THE GPR GRID

The descriptions of the GPR lines indicate that there are a number of sets of structure with very different radar signatures (Fig. 3). These features are: near-surface diffraction patterns (S); two major sub-horizontal reflectors (SHR1 and SHR2); steeply dipping features (DS) above SHR1; and localized shallow-dipping features (SR) below SHR1. The near-surface diffraction patterns (S in Fig. 3) are produced by surface features, such as streams, sediment-filled deformation structures and cracks. Many of the diffraction patterns are asymmetric, as GPR lines do not cross the structures perpendicularly and because the structures are dipping.

Prominent sub-horizontal reflectors

The two prominent sub-horizontal reflectors, SHR1 and SHR2, cannot be seen on the cliff face, as they are both deeper than the interface between the cliff face and the beach sediments deposited at the foot of the ice cliff. The sub-horizontal reflectors could be the expression of any of the following interfaces:

Ice–bedrock interface: Many glacier surveys record strong reflections from the interface between ice and underlying bedrock. However, gravity measurements suggest that bedrock at Kongsvegen is at a depth of many hundreds of metres in the fjord under the calving margin (Oélsner, 1966). Thus, neither reflector is likely to be a bedrock reflection.

Ice–sediment interface: Previous GPR surveys report reflections from an ice–sedimentary-bed interface. Indeed, as Kongsvegen is underlain by sedimentary material in the fjord, such a reflection could be expected and either of the reflectors could represent an ice–sediment interface. Many glaciers also have a thick basal ice zone above the bed, which is recognizable on GPR surveys (Arcone and others, 1995; Murray and others, 2000b). Some deformational features, however, might be expected to cross from the ice into the basal ice. This would argue against SHR1 being an ice–basal-ice reflector, as no reflectors appear to cross the interface.

Thermal boundary in the ice: Radar surveys on polythermal glaciers often record an internal reflection representing the cold-ice–warm-ice transition (cf. Björnsson and others, 1996). Commonly, the thermal boundary is not typically a smooth transition and is represented by increased scatter as a result of diffraction from water-filled voids. The layer at Kongsvegen is a continuous layer so is not thought to be a reflection from a cold–warm thermal interface within ice.

https://doi.org/10.3189/172756503781830458 Published online by Cambridge University Press

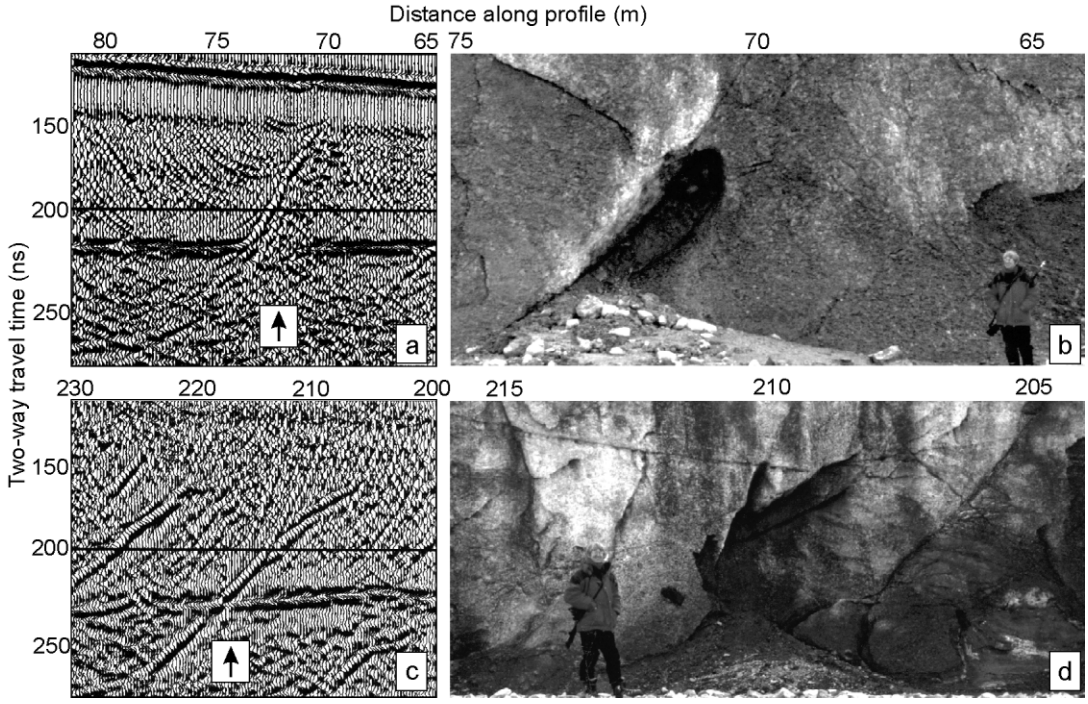

Fig. 4. Dipping reflectors above SHR1 seen in migrated sections (a, c) and in the field (b, d). (a) After migration, the reflector on LL shows a strong, steeply dipping structure, with migration smiles on the up-glacier side of the feature. The reflector shadows any reflection from SHR1 and has no expression below SHR1. From field observations, the feature can be identified as the sedimentary inclusion on the cliff face pictured in (b). The sedimentary structure runs parallel to sedimentary mounds melting out in the forefield. (c, d) Another steeply dipping structure on LL which outcrops on the cliff face. The feature is composed of a series of steeply dipping, sediment-rich fractures, with shallow-angled structures diverging from the main fractures.

Thermal boundary between frozen sediment and unfrozen sediment: In the rapidly thinning, marginal ice of a polythermal glacier, it is possible that the thermal boundary from frozen to unfrozen material might be found in the subglacial sediment, producing a reflective interface.

Brine infiltration: The radar profiles have been collected close to the fjord, so there may be brine infiltration in underlying ice or sediment, which may produce a reflective layer. Kovacs and Gow (1975) mapped a continuous high-amplitude reflector interpreted as resulting from a brine infiltration layer on the McMurdo Ice Shelf, Antarctica. As brine is highly attenuating, no reflectors would be observed below a thick layer of brine, suggesting that neither reflector is produced in this way as clear reflectors are visible below SHR1 and possible reflectors are visible below SHR2.

SHR1 is near-continuous and is the dominant reflector in the profile. No reflectors appear to cross the interface, suggesting that SHR1 is the basal interface between glacier ice and underlying sediment, which represents a plane of décollement. If SHR1 is the glacier bed, then SHR2 is most likely to be a thermal boundary in the sediment below the glacier, particularly as the reflector runs approximately parallel to the glacier surface. In this interpretation, the sediment is frozen above SHR2, while below SHR2 the sediment is unfrozen and assumed to be saturated, producing a detectable reflector. Under this interpretation, no basal ice layer is detectable on the GPR profiles in the marginal zone of Kongsvegen.

Dipping structure above SHR1

The steeply dipping structures on the GPR profiles above SHR1 can be interpreted as representing the sediment-rich structures observed in the cliff face. The series of diffraction patterns below the upper hyperbola result from points where minor sediment-rich structures diverge from the main fracture or from increased sediment inclusions near the bed. These migrate to a point along the plane, which represents the fracture. Proir to migration, the crests of the hyperbolae can be joined to show the location of the fracture, so long as all sediment is in the plane of the profile. The picture is confused where fractures diverge, as reflection points may occur along the splaying fractures. The reflections are further complicated, as many structures appear not to be crossed with the dip of the plane parallel to the GPR profiles.

A number of the sediment-rich fractures can be correlated across adjacent lines of the grid, suggesting that the majority of structures are planar. This is supported by surface mapping of the structures, which shows that most of them are linear at the scale of the GPR grid. Many features at SHR1 continue across two lines and some cross all three. At the surface, fractures can be traced for much longer distances. This suggests that the sediment inclusions are not as continuous as the fractures, and that it is the sediment in the structures that is predominantly responsible for the reflections, and not the fractures themselves. This follows limited evidence from the forefield, which shows short structures, with variable amounts of sediment deposited along ridges, which most likely reflects the availability of sediment during sediment emplacement. The sediment structure shown in Figure 4a and b runs parallel to structures melting out in the glacier forefield. The steeply dipping structure in Figure 4c can also be traced across the GPR lines. The feature is composed of a series of steeply dipping, sediment-rich fractures, with shallow-angled structures diverging from the main fractures, as can be seen in the photograph in Figure 4d.

https://doi.org/10.3189/172756503781830458 Published online by Cambridge University Press

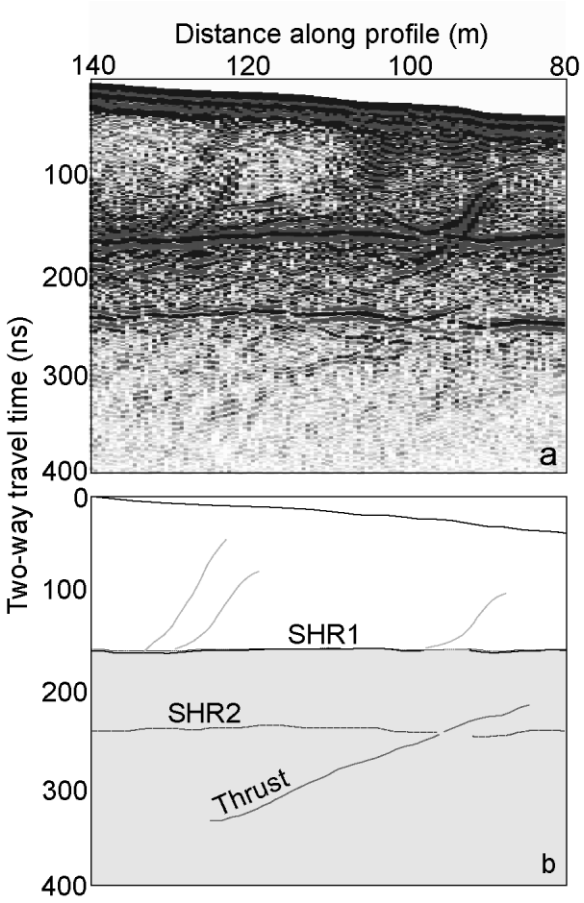

Fig. 5. Dipping reflectors below SHR1: (a) migrated data from LL; (b) interpretation of the migrated GPR plot. The reflector crosses SHR2, where it appears to steepen slightly towards the surface, suggesting that the speed of propagation of electromagnetic waves is slower below SHR2 than above it. These structures are much shallower than the steeply dipping structure found above SHR1, are weaker reflectors and are much less frequent on the GPR traces.

The origin of the sediment within the ice is currently debated. Bennett and others (1996) and Glasser and others (1998) propose that thrusting formed the structures, while Woodward and others (2002) provide an alternative interpretation, suggesting that many of the deformational structures formed by dilated sediments being squeezed into extensional crevasses. These sediment structures were then reorientated within the ice by fast flow during the 1940s surge. No displaced internal layers or structures were observed in the GPR results to support a thrusting mechanism for sediment emplacement. Also, the thrusting models of Bennett and others (1996) and Glasser and others (1998) indicate that the structure should cross the basal interface, so that sediments can be incorporated from the basal environment into the ice. GPR results suggest that this is not the case at Kongsvegen, as no features were imaged that could be traced across SHR1. GPR results therefore support the suggestion by Woodward and others (2002) that the structures are crevasse fills.

Prominent shallow-dipping reflectors at depth in the profile

The 20–30° up-glacier dipping, high-amplitude reflectors below SHR1 are thought to represent thrusts in the subglacial sediment. It seems likely that these thrusts were formed during surge initiation as a result of a compressional regime in the ice of Kongsvegen. Fast-flowing surge ice propagated down-glacier, from a reservoir in the upper basin of Kongsvegen, towards slow-flowing ice in the confluence zone between Kronebreen and Kongsvegen, as was observed at Bakaninbreen (Murray and others, 1998). The ice in the confluence zone was compressed by the surge as it propagated, resulting in Kongsvegen becoming the dominant flow unit at the margin during the surge (Woodward and others, 2002). This produced an initially compressive flow regime for the ice and sediments of Kongsvegen, wherever there was a transition from fast- to slow-moving ice. This transition propagated through the zone of observation, resulting in thrusting.

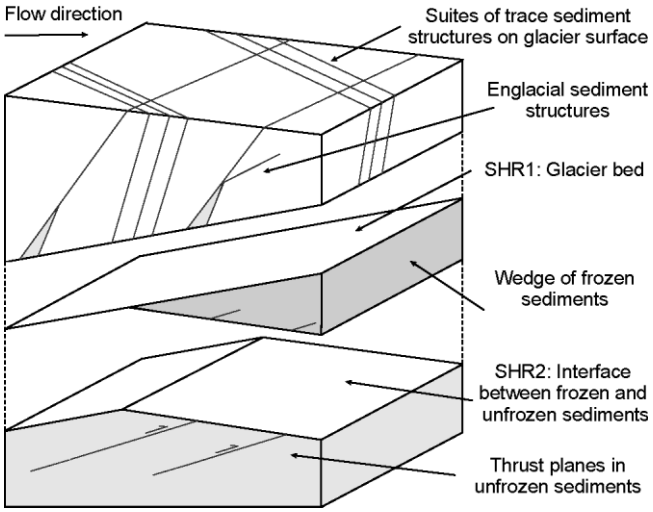

Fig. 6. Schematic summary of GPR results. The subsurface has been divided and separated by the dominant sub-horizontal reflectors SHR1 and SHR2. In the glacier ice above SHR1, schematic sedimentary structures are shown. SHR1 represents the glacier bed, and none of the sedimentary structures appear to cross this interface. Below the bed a frozen wedge of sediment is found, the base of which is defined by SHR2. The sediment is frozen to the base of the glacier by the winter cold wave which penetrates to a depth of ~14 m into glacier ice. The second sub-horizontal interface, SHR2 represents the interface between ice and sediment frozen by the winter cold wave, and underlying, unfrozen, possibly saturated sediment. Some structures appear to cross SHR2. These are interpreted as thrust planes in the subglacial sediments.

The dipping reflectors do not cross SHR1, so during some stage of the surge there must have been a décollement zone between the underlying sediments and the ice. This decoupling of ice from the sediment probably occurred early in the surge (see next section). Thus, the sediment below the SHR1 boundary must have remained largely stationary, or deformed by plug flow, in order to preserve these structures. This suggests deformation of basal sediments in a thin basal zone. Any structure formed in the ice related to the structures in the sediment will have moved down-glacier.

GLACIER SURGE MECHANISMS

The GPR results (summarized in Fig. 6) allow a model for structural development during the surge of Kongsvegen to be proposed:

https://doi.org/10.3189/172756503781830458 Published online by Cambridge University Press

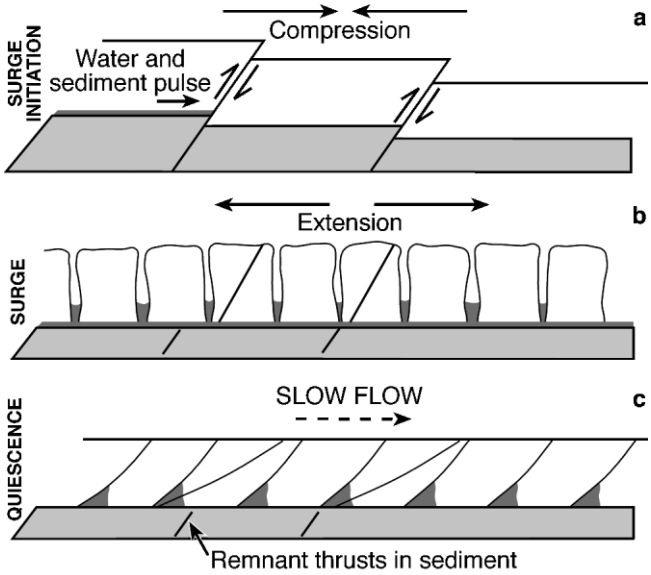

Fig. 7. Schematic showing the development of structure during the surge of Kongsvegen. (a) As the surge front arrives, ice and sediment are thrust due to compression between fast-moving surging ice up-glacier and stagnant ice down-glacier. A water and sediment pulse moves down-glacier with the surge, producing décollement between the ice and sediment. (b) Deforming basal sediments allow fast flow during the surge as the flow regime becomes extensional. (c) Sediments injected into fractures in the ice during the extensional flow regime produce crevasse-fill structures and purge the bed of saturated sediments during surge termination.

1. During surge onset, a compressive regime existed in the ice and basal sediments (Fig. 7). This zone of compression resulted in thrusting of the ice and sediments.
2. With the arrival of fast-flowing ice during the surge, there was a rapid change in some or all of the hydrological, sedimentological or thermal regimes at the basal interface, resulting in decoupling of the ice from the basal sediments.
3. The rapid flow during the surge resulted in the extensive fracture of the ice. Extensional crevasses were the dominant structures on the surface of Kongsvegen after the surge. Voids are likely to have opened in the ice, allowing sediment to be injected from the glacier bed into the ice body.
4. Glaciers flow quickly when lubricated by deforming sediments or water at the bed. Therefore sediment exhaustion from the basal interface due to crevasse filling may have some influence on surge termination. Ensminger and others (2001) suggest that basal crevassing is important for moving sediment above the basal zone of Matanuska Glacier, Alaska, U.S.A., through the injection of turbid water into basal crevasses. At the surge-type Skeiðarárjökull, Iceland, Bennett and others (2000) also suggest that dewatering from basal crevasses may have emplaced sediment in the ice body and have had an influence on the surge. At the surge-type Eyjabakkajökull, Iceland, Sharp (1985) suggests sediment deformation into basal crevasses as the mechanism responsible for producing sediment ridges in the forefield. Sharp (1985) calculates that the crevasse fills removed the equivalent of a layer of sediment 0.16 m thick from the marginal area where the ridges were mapped. This is a significant depth of sediment when compared to the thickness of dilatant layers measured at Breiðamerkurjökull, Iceland (0.4–0.5 m; Boulton and Dent, 1974), and Skalafellsjökull, Iceland (0.5–0.7 m; Sharp, 1984). The GPR surveys suggest that sediment inclusions in Kongsvegen occur at least every 10–15 m, are metres high and are decimetres to metres in width. Reasonable estimates indicate that a depth of sediment of a similar order of magnitude to that found at Eyjabakkajökull could well have been removed from the basal environment at Kongsvegen, indicating that crevasse filling may have been an important mechanism during surge termination, responsible for removing dilated, deforming sediment from the basal environment.

While it is recognized that the GPR data used to construct this model cover a small spatial area of the glacier surface, the results from the GPR are consistent with other observations, suggesting that results can be extrapolated across the catchment. The model has two important implications for the development of the structures in the ice of Kongsvegen. First, it suggests that thrust faulting only occurred during the initial compressive regime. Thrust faults are likely to be difficult to recognize in the current ice, as they will have been moved down-glacier from their expression in the subglacial sediments and also will have been reorientated by velocity gradients within the ice during and after the surge (Woodward and others, 2002). Furthermore, the likely inability of compressive thrust planes to entrain large volumes of sediment suggests they may be difficult to identify as isolated structures in the GPR profiles for the most part. Second, we suggest large amounts of sediment were injected into the ice of Kongsvegen into voids opened by extensional crevasses. Thus most of the structure visible in the ice in the marginal areas of Kongsvegen is thought to originate from crevasse filling.

Studies of surge-type glaciers, which oscillate between short periods of extremely rapid movement and long periods of relative inactivity or quiescence, suggest that fast flow is associated with basal conditions (Clarke and others, 1984; Kamb, 1987; Raymond, 1987). In the case of surge-type glaciers overlying a sedimentary bed, a rapidly deforming, saturated, sediment substrate may induce and/or support surging (Clarke and others, 1984). Surge-type glaciers overlying sedimentary beds often entrain large amounts of sediment (Clapperton, 1975). Therefore, the mechanisms by which sediment is incorporated into the ice during surge may play a significant role in the speed of termination of fast flow by controlling the time taken to reduce the availability of basal sediment and water. The model proposed above suggests that some of the mechanisms that drove the surge of Kongsvegen can be elucidated from studies of the englacial and subglacial sedimentary structures. The termination of the surge may have been assisted by the change in basal conditions when saturated sediments, which had supported fast flow, were injected into open crevasses.

CONCLUSIONS

GPR investigations near a grounded cliff face at the margins of Kongsvegen have enabled the identification of a number of internal reflectors, which represent sedimentary structure within the glacier and the underlying sedimentary bed.

https://doi.org/10.3189/172756503781830458 Published online by Cambridge University Press

Reflectors include: the glacier bed; an underlying thermal interface between frozen and unfrozen sediments; steeply dipping structures imaged above the bed, which are interpreted as crevasse fills and correlate with sediment-rich features seen on the cliff face; and shallow structures visible in the sediment below the bed, which are interpreted as thrust planes formed during the compressional phase of the surge.

The GPR results have allowed the development of a model for structural development during the surge of Kongsvegen. During the 1940s, surge ice moved from a reservoir, propagated down-glacier into slow-flowing ice, creating a zone of compression which resulted in thrusting. Remnant thrust faults are recorded in the subglacial sediments. With the arrival of fast-flowing ice during the surge, the sedimentological and hydrological regime at the basal interface changed rapidly, and the ice decoupled from the basal sediments. Rapid flow during the surge resulted in the extensive fracture of the ice. Sediment is thought to have been injected into these extensional crevasses from the glacier bed, exhausting saturated sediments from the basal interface, possibly accelerating surge termination.

As such, this model suggests that thrusting was an important occurrence during the surge of Kongsvegen, but the thrusting was of little consequence in developing sedimentary landforms in the glacier ice or forefield environment. This suggests that the majority of sedimentary structures visible in the glacier ice and forefield were produced by crevasse filling of extensional crevasses opened during the surge, which have been extensively reorientated by flow during and after the 1940s surge of Kongsvegen.

ACKNOWLEDGEMENTS

Research was funded by the Royal Society. J.W. received a University of Leeds scholarship. N. Cox at the U.K. Natural Environment Research Council Arctic Research Base, Ny Ålesund, Svalbard, provided invaluable logistic assistance. The Sysselmann of Svalbard granted permission to carry out research work at Kongsvegen. We wish to thank Scientific Editor J.W. Glen and reviewers C. F. Raymond and J. Kohler for constructive comments.

REFERENCES

Arcone, S. A., D. E. Lawson and A. J. Delaney. 1995. Short-pulse radar wavelet recovery and resolution of dielectric contrasts within englacial and basal ice of Matanuska Glacier, Alaska, U.S.A. *J. Glaciol.*, **41**(137), 68–86.

Bennett, M. R., M. J. Hambrey, D. Huddart and J. F. Ghienne. 1996. The formation of a geometrical ridge network by the surge-type glacier Kongsvegen, Svalbard. *J. Quat. Sci.*, **11**(6), 437–449.

Bennett, M. R., D. Huddart and R. I. Waller. 2000. Glaciofluvial crevasse and conduit fills as indicators of supraglacial dewatering during a surge, Skeiðarárjökull, Iceland. *J. Glaciol.*, **46**(152), 25–34.

Björnsson, H. *and 6 others*. 1996. The thermal regime of sub-polar glaciers mapped by multi-frequency radio-echo sounding. *J. Glaciol.*, **42**(140), 23–32.

Boulton, G. S. and D. L. Dent. 1974. The nature and rates of post-depositional changes in recently deposited till from south-east Iceland. *Geogr. Ann.*, **56A**(3–4), 121–134.

Clapperton, C. M. 1975. The debris content of surging glaciers in Svalbard and Iceland. *J. Glaciol.*, **14**(72), 395–406.

Clarke, G. K. C. 1976. Thermal regulation of glacier surging. *J. Glaciol.*, **16**(74), 231–250.

Clarke, G. K. C., S. G. Collins and D. E. Thompson. 1984. Flow, thermal structure, and subglacial conditions of a surge-type glacier. *Can. J. Earth Sci.*, **21**(2), 232–240.

Dowdeswell, J. A., G. S. Hamilton and J. O. Hagen. 1991. The duration of the active phase on surge-type glaciers: contrasts between Svalbard and other regions. *J. Glaciol.*, **37**(127), 388–400.

Ensminger, S. L., R. B. Alley, E. B. Evenson, D. E. Lawson and G. J. Larson. 2001. Basal-crevasse-fill origin of laminated debris bands at Matanuska Glacier, Alaska, U.S.A. *J. Glaciol.*, **47**(158), 412–422.

Evans, D. J. A. and B. R. Rea. 1999. Geomorphology and sedimentology of surging glaciers: a land-systems approach. *Ann. Glaciol.*, **28**, 75–82.

Fowler, A. C., T. Murray and F. S. L. Ng. 2001. Thermally controlled glacier surging. *J. Glaciol.*, **47**(159), 527–538.

Glasser, N. F., M. J. Hambrey, K. R. Crawford, M. R. Bennett and D. Huddart. 1998. The structural glaciology of Kongsvegen, Svalbard, and its role in landform genesis. *J. Glaciol.*, **44**(146), 136–148. (Erratum: **46**(154), 2000, p. 538.)

Glover, J. M. and H.V. Rees. 1992. Radar investigations of firn structures and crevasses. *Geol. Surv. Can. Pap.* 90-4, 75–84.

Gudmandsen, P. 1975. Layer echoes in polar ice sheets. *J. Glaciol.*, **15**(73), 95–101.

Hagen, J. O., O. Liestøl, E. Roland and T. Jørgensen. 1993. Glacier atlas of Svalbard and Jan Mayen. *Nor. Polarinst. Medd.* 129.

Hambrey, M. J., J. A. Dowdeswell, T. Murray and P. R. Porter. 1996. Thrusting and debris entrainment in a surging glacier: Bakaninbreen, Svalbard. *Ann. Glaciol.*, **22**, 241–248.

Hambrey, M. J., M. R. Bennett, J. A. Dowdeswell, N. F. Glasser and D. Huddart. 1999. Debris entrainment and transfer in polythermal valley glaciers. *J. Glaciol.*, **45**(149), 69–86.

Jezek, K. C., C. R. Bentley and J.W. Clough. 1979. Electromagnetic sounding of bottom crevasses on the Ross Ice Shelf, Antarctica. *J. Glaciol.*, **24**(90), 321–330.

Kamb, B. 1987. Glacier surge mechanism based on linked cavity configuration of the basal water conduit system. *J. Geophys. Res.*, **92**(B9), 9083–9100.

Kovacs, A. and A. J. Gow. 1975. Brine infiltration in the McMurdo Ice Shelf, McMurdo Sound, Antarctica. *J. Geophys. Res.*, **80**(15), 1957–1961.

Lefauconnier, B., J. O. Hagen and J.-P. Rudant. 1994. Flow speed and calving rate of Kongsbreen glacier, Svalbard, using SPOT images. *Polar Res.*, **13**(1), 59–65.

Macheret, Yu. Ya. and A. B. Zhuravlev. 1982. Radio echo-sounding of Svalbard glaciers. *J. Glaciol.*, **28**(99), 295–314.

Melvold, K. and J. O. Hagen. 1998. Evolution of a surge-type glacier in its quiescent phase: Kongsvegen, Spitsbergen, 1964–95. *J. Glaciol.*, **44**(147), 394–404.

Murray, T., D. L. Gooch and G.W. Stuart. 1997. Structures within the surge front at Bakaninbreen, Svalbard, using ground-penetrating radar. *Ann. Glaciol.*, **24**, 122–129.

Murray, T., J. A. Dowdeswell, D. J. Drewry and I. Frearson. 1998. Geometric evolution and ice dynamics during a surge of Bakaninbreen, Svalbard. *J. Glaciol.*, **44**(147), 263–272. (Erratum: **45**(150), 1999, 405.)

Murray, T., G.W. Stuart, M. Fry, N. H. Gamble and M. D. Crabtree. 2000a. Englacial water distribution in a temperate glacier from surface and borehole radar velocity analysis. *J. Glaciol.*, **46**(154), 389–398.

Murray, T. *and 6 others*. 2000b. Glacier surge propagation by thermal evolution at the bed. *J. Geophys. Res.*, **105**(B6), 13,491–13,507.

Nobes, D. C., S. F. Leary, M. P. Hochstein and S. A. Henrys. 1994. Ground penetrating radar of rubble-covered glaciers: results from the Tasman and Mueller Glaciers of the Southern Alps of New Zealand. *Society of Exploration Geophysicists Annual Meeting. Expanded Abstracts* 64, 826–829.

Oélsner, C. 1966. Ergenbnisse von Gravimetermessungen im Kingsbay-Gebeit (Westspitsbergen). *Petermanns Geogr. Mitt.*, **110**(2), 111–116.

Post, A. 1969. Distribution of surging glaciers in western North America. *J. Glaciol.*, **8**(53), 229–240.

Raymond, C. F. 1987. How do glaciers surge? A review. *J. Geophys. Res.*, **92**(B9), 9121–9134.

Robin, G. de Q. 1955. Ice movement and temperature distribution in glaciers and ice sheets. *J. Glaciol.*, **2**(18), 523–532.

Sharp, M. 1984. Annual moraine ridges at Skálafellsjökull, south-east Iceland. *J. Glaciol.*, **30**(104), 82–93.

Sharp, M. 1985. "Crevasse-fill" ridges — a landform type characteristic of surging glaciers? *Geogr. Ann.*, **67A**(3–4), 213–220.

Woodward, J., T. Murray and A. McCaig. 2002. Formation and reorientation of structure in the surge-type glacier Kongsvegen, Svalbard. *J. Quat. Sci.*, **17**(3), 201–209.

MS received 25 October 2002 and accepted in revised form 21 July 2003